Available online at www.sciencedirect.com

SCIENCE DIRECT

Biochimica et Biophysica Acta 1708 (2005) 42–49

BIOCHIMICA ET BIOPHYSICA ACTA BBA

http://www.elsevier.com/locate/bba

EPR properties of a g=2 broad signal trapped in an S_1 state in Ca^{2+}-depleted Photosystem II

Hiroyuki Mino*, Shigeru Itoh

Division of Material Science (Physics), Graduate School of Science, Nagoya University, Furocyo, Chikusa, Nagoya 464-8602, Japan

Received 8 August 2004; received in revised form 18 December 2004; accepted 6 January 2005
Available online 25 January 2005

Abstract

We investigated a new EPR signal that gives a broad line shape around g=2 in Ca^{2+}-depleted Photosystem (PS) II. The signal was trapped by illumination at 243 K in parallel with the formation of $Y_Z^{\bullet}$. The ratio of the intensities between the g=2 broad signal and the $Y_Z^{\bullet}$ signal was 1:3, assuming a Gaussian line shape for the former. The g=2 broad signal and the $Y_Z^{\bullet}$ signal decayed together in parallel with the appearance of the S_2 state multiline at 243 K. The g=2 broad signal was assigned to be an intermediate $S_1X^{\bullet}$ state in the transition from the S_1 to the S_2 state, where $X^{\bullet}$ represents an amino acid radical nearby manganese cluster, such as D1-His337. The signal is in thermal equilibrium with $Y_Z^{\bullet}$. Possible reactions in the S state transitions in Ca^{2+}-depleted PS II were discussed.

Keywords: Ca^{2+} depletion; Manganese cluster; Oxygen evolving complex; Photosystem II; Split EPR signal

1. Introduction

Photosynthetic oxygen evolution is carried out by a machinery termed oxygen-evolving complex (OEC). OEC is composed of four manganese ions, one calcium ion, chloride, and Y_Z tyrosine and is located at the lumenal surface of the Photosystem (PS) II D1 reaction center protein. Recently, PS II structures with 3.5–3.7 Å resolutions have been reported [1–3]. The four Mn ions form a tetranuclear cluster that accumulates oxidized equivalents generated in the PS II reaction center by the successive absorption of four photons to catalyze water oxidation. Kinetic analyses have revealed that a molecular oxygen is produced by a series of reactions with five distinct intermediate states labeled S_i (i=0–4), in which S_1 is thermally stable in the dark. As photons are absorbed by the reaction center, the S state advances stepwise to reach the S_4 state, which is the highest oxidation state. S_4 decays spontaneously to S_0 by releasing molecular oxygen [as reviewed in Refs. [4–7]].

EPR is a powerful tool that provides structural and functional information about the OEC. After the first discovery of the S_2 state multiline signal [8], many EPR signals from the different states of the OEC have been reported. The EPR signal of the S_0 state, which shows a hyperfine structure that is similar to the multiline signal in the S_2 state but with a broader overall width, was assigned to the antiferro-magnetically coupled S=1/2 system in the ground state [9,10]. S_1 and S_3 state EPR signals with broad linewidths were also identified in spinach PS II and assigned to a first excited state S=1 of an integer spin system [11–13]. On the other hand, in PS II preparations of *Synechocystis* sp. and spinach, which are depleted of 23 and 17 kDa extrinsic polypeptides, a different S_1 state signal with a hyperfine structure was observed [14,15]. Nugent et al. have reported an EPR signal at g=2 that is produced by illumination below 20 K of the S_1 state in untreated PS II and ascribed it to $S_1X^{\bullet}$ [16]. The $S_1X^{\bullet}$ signal decays after dark annealing at 77 K with the appearance of a multiline signal. Illumination at 5

Abbreviations: CW, continuous-wave; DCMU, 3-(3,4-dichlorophenyl)-1,1-dimethylurea; EDTA, ethylene diamine tetraacetic acid; EPR, electron paramagnetic resonance; ENDOR, electron nuclear double resonance; MES, 2-morpholinoethanesulfonic acid; MOPS, 2-(*N*-morpholino)ethane-sulfonic acid; OEC, oxygen-evolving complex; PS, photosystem; Y_Z, tyrosine-Z, the D1-Tyr161; Y_D, tyrosine-D, the D2-Tyr161

* Corresponding author. Fax: +81 52 789 2883.
E-mail address: mino@bio.phys.nagoya-u.ac.jp (H. Mino).

0005-2728/$ - see front matter © 2005 Elsevier B.V. All rights reserved.
doi:10.1016/j.bbabio.2005.01.001

K, on the other hand, induced two different types of g=2 EPR signals, depending on the S state [17]. A model for the interaction of the S_1 state and the $Y_Z^{\bullet}$ radical has been proposed on the basis of the analogy with a model, in which the "split signal" arises from the interaction between the S_2 state and the $Y_Z^{\bullet}$ radical [18].

Calcium is indispensable for the normal function of OEC. The oxygen evolution is inhibited by the selective depletion of Ca^{2+} and is restored by the reconstitution of Ca^{2+} [19]. Ca^{2+} has been assumed to play a structural role, such as the stabilization and optimization of the Mn-cluster, and/or to participate directly in the water-oxidation reaction. The depletion of Ca^{2+} or its replacement by other metal cations modifies the properties of the Mn-cluster in the S_2 state, depending on the metal ions in the process of Ca^{2+} depletion [20–23]. The illumination of the Ca^{2+}-depleted PS II in the S_2 state generates another EPR signal with a splitting linewidth of 160 gauss around g=2 with complete or partial disappearance of the S_2 state multiline signal [24]. This split signal has been denoted as the "S_3'-state signal." The S_3'-state signal was ascribed to be formed by an auxiliary reaction in PS II, in which the $Y_Z^{\bullet}$ radical was stabilized by the interruption of the normal oxidation process to the S_3 state in the absence of Ca^{2+}. There have been two alternative interpretations for the origin of the split signal. The first is that the g=2.0 split signal arises from an organic radical with S=1/2 that interacts with an oxidized Mn-cluster with S=1/2 (S_2 state). In this case, an oxidized histidine [25,26] or $Y_Z^{\bullet}$ [27] has been attributed to the putative radical. The signal has been interpreted to arise from the interaction between the $Y_Z^{\bullet}$ radical and the oxidized Mn-cluster (S=1), based on a simulation of the ESE-field swept spectrum in Ca^{2+}-depleted PS II by assuming a 4.5 Å inter-distance between these species [28]. It is alternatively assumed that the signal arises from the interaction between the $Y_Z^{\bullet}$ radical and the S_2-state Mn-cluster (S=1/2). This is based on the simulation of the ESE field-swept spectrum measured in acetate-treated PS II by assuming a distance of 3.5 Å between $Y_Z^{\bullet}$ and $(Mn)_4$ [29]. The involvement of the $Y_Z^{\bullet}$ radical in the split signal has also been suggested by the pulsed ENDOR and ESEEM results obtained in acetate-treated PS II [28,30]. It is notable that the split signal has been assumed to arise from a single magnetic species in these studies.

The other interpretation of the split signal has been based on the finding that the split signal consists of two overlapping different signals: a symmetric doublet signal and an asymmetric singlet-like signal [31]. The doublet signal has a splitting of approximately 150 G at g=2 and is induced by the illumination of the Ca^{2+}-depleted PS II in the S_2 state in the presence of DCMU or by a short period of illumination at 273 K in the absence of DCMU. The singlet-like signal is induced by illumination for a longer period and suppressed in the presence of DCMU. The formation of this signal, therefore, requires more than two turnovers of the PS II light reaction, which advances OEC beyond the S_2 state. The doublet signal has been simulated by assuming D_0=130 G and J=(−) 40 G for a typical interaction, called Pake's doublet, between paired organic radicals [31]. The anisotropy of the doublet signal that is expected for the paired organic radicals was also confirmed by ESE measurements in oriented PS II membranes [32]. The results of a pulsed ENDOR-induced EPR study indicate that the $Y_Z^{\bullet}$ radical is associated with the doublet signal but not with the singlet-like signal [31]. These results suggest that the doublet signal arises from a dipole interaction between the $Y_Z^{\bullet}$ radical and another organic radical [31], while the origin of the singlet-like signal is not clear yet. The g=11–15 signal with an S=2 spin state was also observed in parallel with a singlet-like signal [33]. The intensity of the doublet signal is independent from that of the multiline signal; thus, the doublet signal cannot be directly related to the manganese cluster [34]. Based on these observations, the relative locations of the two radicals responsible for the doublet signal were estimated [32].

In the present study, we report a new EPR signal at a g=2 region detected in the illuminated S_1 state in Ca^{2+}-depleted PS II. Based on the structure of the PS II reaction center [3], we discuss the origin of the so-called "split signal."

2. Materials and methods

Oxygen-evolving PS II membranes were prepared from spinach as described previously [35] with some modifications [36]. After being thawed, the membranes were pre-illuminated and relaxed by incubation for 12 h in the dark. The membranes were washed twice in a medium containing 400 mM sucrose, 20 mM NaCl, and 0.1 mM MES/NaOH (pH 6.5) and were resuspended in the same medium. For Ca^{2+} depletion, the membranes were suspended in a medium containing 400 mM sucrose, 20 mM NaCl, and 10 mM citric acid/NaOH (pH 3.0) for 5 min at 273 K; then, 10 vol.% of a medium containing 400 mM sucrose, 20 mM NaCl, and 500 mM MOPS/NaOH (pH 7.5) was added to adjust the final pH to approximately 6.5, as described previously [37]. The membranes were washed twice in a medium containing 400 mM sucrose, 20 mM NaCl, 20 mM Mes/NaOH (pH 6.5), and 0.5 mM EDTA. Unless otherwise stated, all procedures were carried out in the dark or under a dim green light to maintain the OEC in the S_1 state. DCMU (dissolved at 10 mM in dimethyl sulfoxide) was added to give a final concentration of 0.05 mM in the dark to the S_1 state PS II.

For the EPR measurement, the membranes were precipitated by centrifugation at 35,000×g for 20 min and transferred to suprasil quartz EPR tubes with a 4-mm diameter. The tubes were purged with Ar gas, sealed, and then stored in liquid N_2 until use. The PS II sample in an ESR tube was illuminated for 10 s with a 500 W halogen–tungsten lamp in an ethanol bath at 243 K and then rapidly frozen in liquid N_2 just after the illumination.

EPR measurements were performed by using a Bruker ESP-300 EPR spectrometer equipped with a standard resonator (ER4102). A gas flow temperature control system (CF935, Oxford Instruments) was used.

3. Results

Fig. 1 shows the effect of illumination at low temperature of the Ca^{2+}-depleted PS II membranes. The Ca^{2+}-depleted PS II membranes in the S_1 state (trace a) were illuminated for 3 min at 200 K in the presence of DCMU (trace b). The difference spectrum (trace d) shows the formation of the Q_A^- signal and a subtle featureless signal around g=2 with a 100–130 G width (trace d, array). Trace c shows the signal after dark annealing for 30 min at 273 K (trace b). For comparison, Trace e shows the difference spectrum of the S_1 state and S_2 state illuminated for 3 min at 200 K in untreated PS II. The g=2 broad signal decayed, and the alternative S_2 multiline signal was formed. The Q_A^- signal intensities did not change, indicating that the formation of the multiline after dark annealing can be ascribed to the conversion only in the donor side of PS II.

Fig. 2 shows that the $Y_Z^{\bullet}$ signal and g=2 broad signal decay in parallel and occurred concomitantly with the appearance of the S_2 multiline signal after the dark annealing at 243 K. Panel A shows the EPR spectra of the Ca^{2+}-depleted PS II membranes that were illuminated for 10 s at 243 K (trace a) and dark annealed for 30 s (trace b) and 150 s (trace c) at 243 K in the presence of DCMU. Panel B shows the EPR spectra of the g=2 region after illumination for 10 s at 243 K (trace d) and dark annealing for 150 s at 243 K (trace e) and the difference between them (trace f). The $Y_Z^{\bullet}$ species is known to be trapped at a 50–60% yield by the 243 K illumination in Ca^{2+}-depleted PS II [38,39]. The $Y_Z^{\bullet}$ signal shows a slightly broader line shape compared to the Y_D signal. We have previously reported that the $Y_Z^{\bullet}$ signal is dependent on pH [39,40]. The ENDOR results show that the pH dependence is not caused by the broadening of a neutral radical form but by the modification of the spin distribution on the radical (cation-like signal) [39,40]. Fig. 3 shows the decays of these signals during annealing at 243 K. The extent of the difference between the sample measured immediately after illumination and annealed for 30 min at 273 K was compared. The decays of the $Y_Z^{\bullet}$ and the g=2 broad signals proceeded in parallel and concomitantly with the formation of the multiline signal. All three processes gave the same time constants $t_{1/2}$ of ~50 s. The results indicate the conversion of the Y_Z radical to the multiline after dark annealing and confirm the early reports that showed the quantitative relationship between the extents of the Y_Z radical and the multiline signal [38]. In addition, we can also identify the g=2 broad signal, which was ignored in the previous report [38]. The wide linewidth of the g=2 broad signal shows that it does not arise from a simple organic radical. It seems to arise from a metal center or some species broadened by magnetic interaction. Similar EPR signals have been observed in inhibited PS II membranes with the name of "split signal" [20,21,23–25,28–30,41–43]. The split signals have been

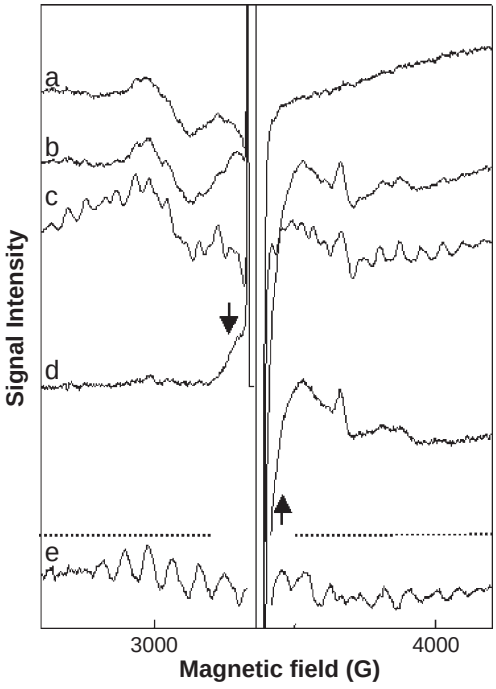

Fig. 1. CW EPR spectra of Ca^{2+}-depleted PS II membranes in the presence of DCMU in the S_1 state after illumination at 200 K (traces a–d). The membranes in the S_1 state (trace a) were illuminated for 3 min at 200 K (trace b) and dark-adapted for 30 min at 273 K (trace c). Trace d is the difference spectrum of traces a and b. Trace e is the difference spectrum between the S_2 and S_1 state in untreated PS II membranes. The S_2 state was produced by illumination for 3 min at 200 K. EPR conditions: microwave power, 0.2 mW; field modulation amplitude, 20 G at 100 kHz; scan time, 168 s; time constant, 0.3 s; temperature, 6 K.

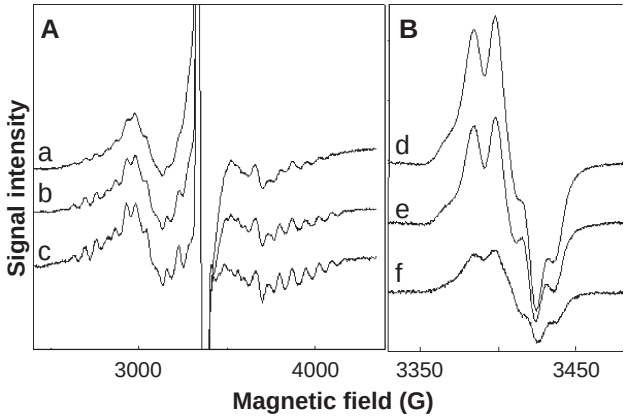

Fig. 2. Effect of dark adaptation on the intensities of the multiline signal and the $Y_Z^{\bullet}$ signal after illumination at 243 K in Ca^{2+}-depleted PS II membranes in the S_1 state in the presence of DCMU. Ca^{2+}-depleted PS II membranes were illuminated for 10 s (traces a and d) and dark-adapted for 30 s (trace b) and 150 s (traces c and e) at 243 K. Trace f is a difference spectrum of traces d and e. EPR conditions: microwave power, 0.2 mW (traces a–c) and 0.63 μW (traces d–f); field modulation amplitude, 20 G (traces a–c) and 4 G (traces d–f) at 100 kHz; scan time, 168 s; time constant, 0.3 s; temperature, 6 K.

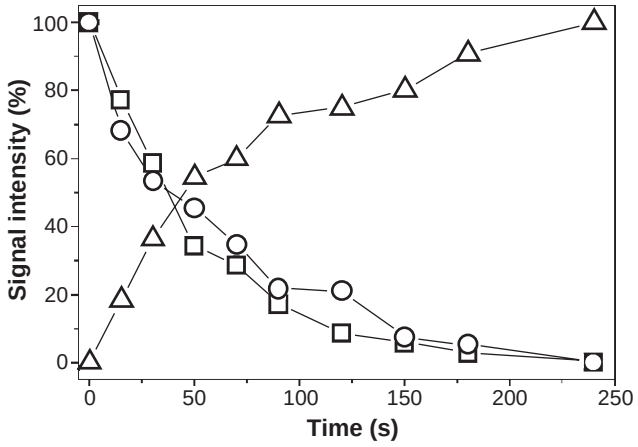

Fig. 3. Effects of dark incubation on the extents of the g=2 broad signal (○), $Y_Z^{\bullet}$ signal (□), and multiline signal (△). Ca^{2+}-depleted PS II membranes stored in the presence of DCMU in the S_1 state were illuminated for 10 s at 243 K and then dark-incubated at 243 K as indicated in the figure.

proposed to arise from a state that is oxidized beyond S_2 in the inhibited samples, such as acetate-treated or ammonium-treated PS II, in analogy to the case of Ca^{2+}-depleted PS II.

Fig. 4 shows the light-minus-dark spectrum of the g=2 broad signal trapped after 10 s illumination at 243 K (trace a) and its integrated spectrum (trace b). The central over-scaled part of the spectrum represents the overlapped tyrosine signals with a narrower bandwidth. Although the accurate line shape of the g=2 broad signal is unclear because of overlapped tyrosine radicals, the signal shows

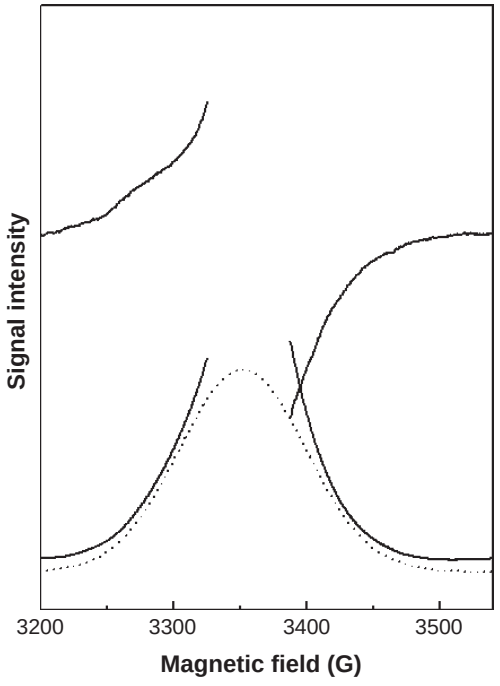

Fig. 4. Spectra of the g=2 broad signal (trace a) and its integration (trace b). The signal was obtained by subtracting the S_1 state background signal. The dotted line (trace c) represents the fitted Gaussian line shape assuming a width of 111 G. See the text for details. The EPR conditions are the same as those in Fig. 1, except for the temperature of 15 K.

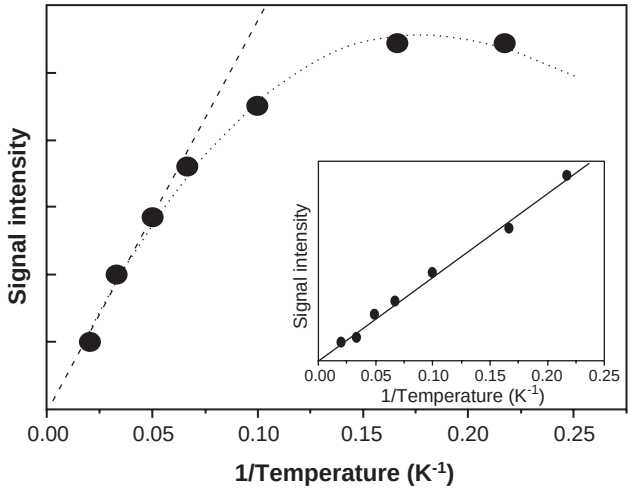

Fig. 5. Temperature dependence of the intensity of the g=2 broad signal. The dotted line shows the case of linear correlation between the (temperature)$^{-1}$ and the signal intensity. The broken line shows the correlation based on the interaction model (see text). The inset shows the temperature dependence of tyrosine radicals ($Y_Z^{\bullet}$ +$Y_D^{\bullet}$).

broad and good symmetrical line shapes. We can estimate the approximate signal intensity of the signal in the unresolved resonance spectrum based on the line shapes of the integrated spectrum. Gaussian line shapes are assumed. Trace c shows the Gaussian fitting curve with a 110 G width around g=2. The integrated intensity of the simulated g=2 broad signal was 33% of that of the Y_Z radical, which was, in turn, 50% of the Y_D radical trapped at the same time.

Fig. 5 shows the temperature dependence of the signal intensities of g=2 and the tyrosine radical. The intensity of the g=2 broad signal was evaluated from the light-minus-dark spectra measured under a non-saturating microwave power. The temperature dependence of the g=2 broad signal shows non-Curie-law behavior below 10 K. The inset showed the Curie-law behavior of the temperature dependence of the tyrosine radicals ($Y_Z^{\bullet}$ +$Y_D^{\bullet}$). The results suggest that the g=2 broad signal is related to the excited state of the interacting spin system. Assuming a simple spin-exchange interaction model $-2JS_A \cdot S_B$ (S=1/2 for S_A,S_B), J is estimated to be 27 cm^{-1}.

4. Discussion

4.1. Origin of the g=2 broad signal trapped in the S_1 state

We have shown the behavior of a new signal with a broad linewidth around g=2 in Ca^{2+}-depleted PS II in the S_1 state. The decrease of the g=2 broad signal followed the same time course as that of the increase of the S_2 multiline, suggesting that the signal is the intermediate state between the S_1 and S_2 states. At first, we tentatively denoted the state of the g=2 broad signal as [S_{1ox}]. On the other hand, it is clear that the trapped $Y_Z^{\bullet}$ radical oxidizes the S_1 state and forms the S_2

multiline in the main reaction of OEC. The decay of the Y_Z radical was in parallel with the decay of the g=2 broad signal. This shows that these two reactions proceed in parallel (Scheme 1), where $S_1Y_Z^{\bullet}$ (trapped Y_Z radical) is in a thermodynamic equilibrium with $[S_{1OX}]Y_Z$ (g=2 broad signal). Based on the ratio of the signal intensities, the ratio of $Y_Z^{\bullet}$:$[S_{1ox}]$ equilibrium is estimated to be about 3:1. This gives a G value of about 2 kJ/mol at 243 K.

We assume that the g=2 broad signal arises from the interaction between the manganese cluster in the S_1 state and a nearby oxidized radical $X^{\bullet}$, denoted as $S_1X^{\bullet}$. The spin interactions are described by the exchange interaction J and the magnetic dipole interaction D. J is the isotropic interaction, expressed as the overlapping of the molecular orbitals [44]. D is an isotropic interaction, expressed as $\mu_1\mu_2/r^6$, where μ and r represent the magnetic moment and inter-distance of the two magnetic moments, respectively. In the case of weak coupling ($J \ll D$), we can estimate the distance between spins based on the dipole interaction D. If the g=2 broad signal arises from a weak coupling of S_1 with $X^{\bullet}$, the distance r between two spins is estimated as 6.3 Å, assuming S=1 for the S_1 state, S=1/2 for $X^{\bullet}$, and an internal linewidth of 20 G for $\dot{X}$ [45]. We can evaluate the distance as the upper-limit because the closer distance can be estimated in the case of intermediate or strong couplings ($J \geqq D$). The Y_Z radical signal without noticeable line-broadening was observed in the presence of the manganese cluster in conventional EPR measurements. This indicates that the distance between $Y_Z^{\bullet}$ (S=1/2) and the manganese cluster (S=1) is more than 10 Å. Therefore, the origin of the g=2 broad signal does not seem to reflect the interaction between $Y_Z^{\bullet}$ and the manganese cluster. These considerations are essentially consistent with those in earlier reports [38].

4.2. Relationship between the broad signal and other signals detected in Ca^{2+}-depleted PS II

We have reported two split signals in Ca^{2+}-depleted PS II, namely, doublet and singlet-like signals [32,33]. Fig. 6 shows (a) the g=2 broad signal, (b) the doublet signal, and (c) the singlet-like signal. The doublet signal has a 160 G symmetrical line shape around g=2. It was produced by short or long illumination in the presence of DCMU in the S_2 state at 273 K. The singlet-like signal gives an asymmetrical line shape around g=2 and is formed only after long illumination. The exact line shape of the singlet-like signal is unknown because of the overlapping of the doublet signal. ENDOR-induced EPR data have shown that the doublet signal originates from two radicals, the Y_Z radical and a nearby amino-acid radical $\dot{R}$ that interacts with the Y_Z radical but not with the S_2 multiline state [31]. The behavior of a doublet signal that is independent from that of the manganese cluster supports this model [34]. On the other hand, the singlet-like signal seems to originate from the interaction of the manganese cluster with the nearby radical $\dot{X}$ [33]. The signal has a wide and asymmetrical EPR line shape compared to the signals of ordinary organic radical species. Furthermore, the g=11–15 signal with an S=2 spin state and the singlet-like signal can be observed to have the same time course [33].

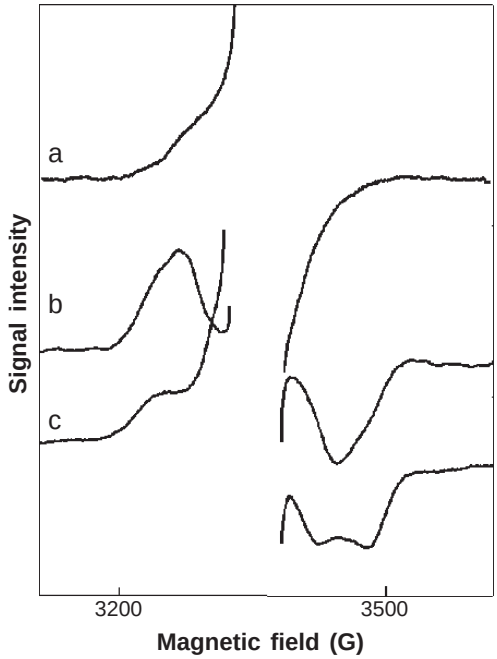

Fig. 6. CW EPR spectra of the g=2 broad signal (trace a), the doublet signal (trace b), and the singlet-like signal (trace c) in Ca^{2+}-depleted PS II membranes. The g=2 broad signal was produced by illumination for 10 s at 243 K in the presence of DCMU. The doublet signal was produced by illumination for 60 s at 273 K in the presence of DCMU. The singlet-like signal was produced by illumination for 60 s at 273 K in the absence of DCMU. Spectra are shown after subtracting the S_1 spectrum. EPR conditions: microwave power, 0.2 mW; field modulation amplitude, 20 G at 100 kHz; scan time, 168 s; time constant, 0.3 s; temperature, 6 K.

In the simplest case, we can assume that the same radical $X^{\bullet}$ is responsible for the g=2 broad signal $[S_{1ox}]$ and for the singlet-like signal. The different line shape of these two signals may be explained by the different spin state of the interacting manganese cluster. If we assume that the radical $X^{\bullet}$ interacts with the manganese cluster in the S_3 state Ca^{2+}-depleted PS II, the asymmetrical line shape of the singlet-like signal may be explained by the interaction between the radical $X^{\bullet}$ and asymmetrical g=11–15 (S=2) signal [33]. The reaction model in Ca^{2+}-depleted PS II is summarized in Scheme 2.

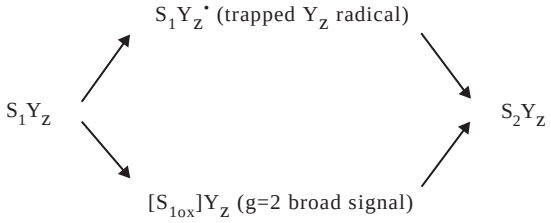

Scheme 1. Redox Events between S_1–S_2 states transition in Ca^{2+}-depleted PSII.

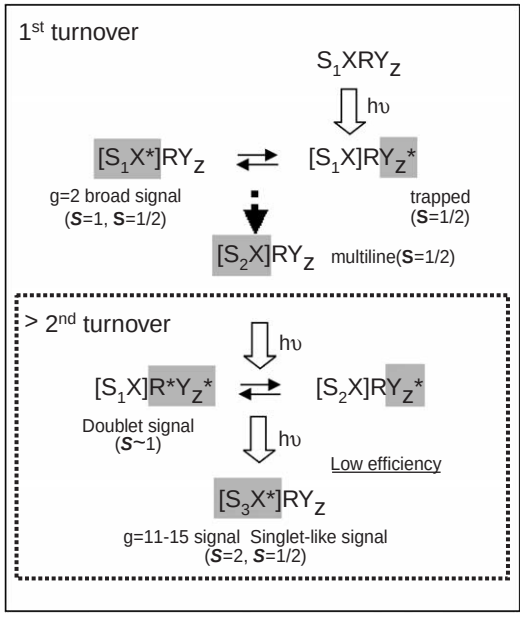

Scheme 2. Redox Events in OEC caused by illuminating Ca^{2+}-depleted PSII.

4.3. Comparison with broad signals detected around g=2 in untreated and treated PS II

Recently, a similar signal at g=2 was reported to be formed in the S_1 state in untreated PS II by illumination at 5 K [16]. We also tried to trap this signal by illumination at 10 K in Ca^{2+}-depleted PS II but did not succeed (data not shown), probably due to the difference in the temperature dependence of the Y_Z oxidation [38]. The g=2 broad signal in the untreated S_1 state might occur by the same mechanism as that of the g=2 broad signal in S_1 state Ca^{2+}-depleted PS II. Zhang and Styring have reported two types of "split signals" in untreated PS II [17]. It might be consistent with the conclusion of the present study in Ca^{2+}-depleted PS II that the split signal represents more than two species. However, the origin and mechanism of the signals are not clear in untreated PS II. Koulougliotis et al. showed the temperature dependence of the broad signal in untreated PS II and suggested it to be a ground state or a weakly excited state [18]. We can speculate that the differences in the formation temperature and the temperature dependence of the signal intensity reflect the modification of OEC in Ca^{2+}-depleted PS II, in which the electron donation to OEC was inhibited below 220 K, the S_1 signal was undetected, and the S_2 multiline was abnormally stable [46].

4.4. Comparison of the EPR results with the structure of Photosystem II

X-ray studies have revealed the structure of PS II at 3.5 Å resolution [3]. Although the resolution is not sufficient to clarify the origin of the EPR signals, it is worth comparing the structure with the orientation and the mutual distances of radicals obtained by EPR measurements. Note that the distances estimated by EPR are those between centers of electronic spins. The distance between the center of the aromatic ring in Y_Z and each manganese atom was estimated to be about 10 Å based on X-ray coordination data [3]. Since an overlapping of molecular orbitals is expected to be low between the manganese cluster and Y_Z, D should be much larger than J. If we assume the interaction between the manganese cluster and the nearby amino-acid radical $\dot{X}$, the distance of 6.5–8 Å estimated by the EPR linewidth is almost consistent with the distance estimated in some kinds of split signals [45,47]. Only a few candidate residues for X in the PS II structure can be assumed [3]. His 337 seems to be a good candidate of X, which gives distances of 5–7.7 Å between each manganese ion and the center of its imidazole ring. However, there is no other spectroscopic evidence to support this assumption.

4.5. Origin of the doublet signal

The neutral radical pair $Y_Z^{\bullet}$–$R^{\bullet}$ has been estimated to be the origin of the doublet signal, and R has been proposed as a redox-active amino-acid residue [31]. The distance between the ring centers of Y_Z and R has been estimated to be 5.3 Å [32,33], together with their relative positions on the membrane [32]. A few candidates for R can be assumed based on the structural data [3]. The angle between the membrane normal and the vector of Y_Z–His190 was estimated to be 69° [3], while the angle between the membrane normal and the dipole-vector in the doublet signal was estimated to be 65° [32]. The angle between both vectors in the membrane plane was 64° [32]. The angles between the radius vectors of the radical pair with Y_D and the membrane plane were 8° in the doublet signal and 4.5° in the Y_Z–His190 pair [32]. Based on these consistencies, His190 can be a good candidate for R as a partner of Y_Z to form a doublet signal. This is consistent with earlier reports that showed the involvement of the His radical in the split signal [23,26]. Discussions have also taken place concerning whether or not His190 is hydrogen-bonded with Y_Z. The H-bonding of His190 to Y_Z might be important in proton transfer in the H_2O oxidation process [48]. We have previously reported the pH dependence of the Y_Z signals in Mn-depleted PS II [40] and in Ca^{2+}-depleted PS II [39]. In Mn-depleted PS II, the $Y_Z^{\bullet}$ has a neutral radical form above pH 6.5 and a modified (cation-like) form below pH 6.5. In Ca^{2+}-depleted PS II, $Y_Z^{\bullet}$ had a cation-like form at pH 6.5, and the mixture of neutral and cation-like signals took place at pH 7.0. Furthermore, $Y_Z^{\bullet}$ included in the doublet signal was also in a neutral form in both pH 5.5 and pH 7.0. These pH dependences might be caused by electrostatic modification of the Y_Z surroundings induced by the protonation of His190. Although it is not clear why His190 is oxidized in a specified condition, the EPR signal can be a useful tool to study the mechanism of

oxygen evolution. The features of a broad g=2 signal and the pathway proposed in the present study indicate the important role of amino acid residues in OEC.

Acknowledgements

This research was supported by grants No. 15370067 to S. I. and the 21st Century COE program, "The Origin of the Universe and Matter," of Nagoya University from MECSST of Japan.

References

[1] A. Zouni, H.T. Witt, J. Kern, P. Fromme, N. Krauss, W. Saenger, P. Orth, Crystal structure of Photosystem II from *Synechococcus elongatus* at 3.8 Å resolution, Nature 409 (2001) 739–743.
[2] N. Kamiya, J.R. Shen, Crystal structure of oxygen-evolving Photosystem II from *Thermosynechococcus vulcanus* at 3.7-angstrom resolution, Proc. Natl. Acad. Sci. U. S. A. 100 (2003) 98–103.
[3] K.N. Ferreira, T.M. Iverson, K. Maghlaoui, J. Barber, S. Iwata, Architecture of the photosynthetic oxygen-evolving center, Science 303 (2004) 1831–1838.
[4] R.J. Debus, The manganese and calcium—Ions of photosynthetic oxygen evolution, Biochim. Biophys. Acta 1102 (1992) 269–352.
[5] A.W. Rutherford, J.-L. Zimmermann, A.T.P. Boussac, Structure, Function and Molecular Biology, Elsevier, Amsterdam, 1992.
[6] K. Sauer, V.K. Yachandra, R.D. Britt, M.P. Klein, Manganese Redox Enzymes, VCH, New York, 1992.
[7] B. Ke, The Photosynthesis: Photobiochemistry and Photobiophysics, Kluwer, The Netherlands, 2001.
[8] G.C. Dismukes, Y. Siderer, Intermediates of a polynuclear manganese center involved in photosynthetic oxidation of water, Proc. Natl. Acad. Sci. 78 (1981) 274–278.
[9] J. Messinger, J.H. Robblee, W.O. Yu, K. Sauer, V.K. Yachandra, M.P. Klein, The S_0 state of the oxygen-evolving complex in Photosystem II is paramagnetic: detection of EPR multiline signal, J. Am. Chem. Soc. 119 (1997) 11349–11350.
[10] K.A. Ahrling, S. Peterson, S. Styring, An oscillating manganese electron paramagnetic resonance signal from the S_0 state of the oxygen evolving complex in Photosystem II, Biochemistry 36 (1997) 13148–13152.
[11] S.L. Dexheimer, M.P. Klein, Detection of a paramagnetic intermediate in the S1-state of the photosynthetic oxygen-evolving complex, J. Am. Chem. Soc. 114 (1992) 2821–2826.
[12] T. Yamauchi, H. Mino, T. Matsukawa, A. Kawamori, T. Ono, Parallel polarization electron paramagnetic resonance studies of the S_1-state manganese cluster in the photosynthetic oxygen-evolving system, Biochemistry 36 (1997) 7520–7526.
[13] T. Matsukawa, A. Kawamori, H. Mino, Electron paramagnetic resonance study of the magnetic structure of the S_1-state in oriented oxygen evolving Photosystem II membranes, Spectrochim. Acta, A Mol. Spectrosc. 55 (1999) 895–901.
[14] K.A. Campbell, J.M. Peloquin, D.P. Pham, R.J. Debus, R.D. Britt, Parallel polarization EPR detection of an S_1-state "multiline" EPR signal in Photosystem II particles from *Synechocystis* sp. PCC 6803, J. Am. Chem. Soc. 120 (1998) 447–448.
[15] R.D. Britt, J.M. Peloquin, K.A. Campbell, K. Clemens, M. Evanchik, EPR characterization of the Photosystem II oxygen evolving complex, J. Inorg. Biochem. 74 (1999) 13.
[16] J.H.A. Nugent, I.P. Muhiuddin, M.C.W. Evans, Electron transfer from the water oxidizing complex at cryogenic temperatures: the S-1 to S-2 step, Biochemistry 41 (2002) 4117–4126.
[17] C.X. Zhang, S. Styring, Formation of split electron paramagnetic resonance signals in Photosystem II suggests that tyrosine(z) can be photooxidized at 5 K in the S-0 and S-1 states of the oxygen-evolving complex, Biochemistry 42 (2003) 8066–8076.
[18] D. Koulougliotis, J.R. Shen, N. Ioannidis, V. Petrouleas, Near-IR irradiation of the S-2 state of the water oxidizing complex of Photosystem II at liquid helium temperatures produces the metal-loradical intermediate attributed to $S_1Y_Z^{\cdot}$, Biochemistry 42 (2003) 3045–3053.
[19] T. Ono, Y. Inoue, Discrete extraction of the Ca atom functional for O_2 evolution in higher-plant Photosystem-Ii by a simple low pH treatment, FEBS Lett. 227 (1988) 147–152.
[20] M. Sivaraja, J. Tso, G.C. Dismukes, A calcium-specific site influences the structure and activity of the manganese cluster responsible for photosynthetic water oxidation, Biochemistry 28 (1989) 9459–9464.
[21] J. Tso, M. Sivaraja, J.S. Philo, G.C. Dismukes, Ca^{2+} depletion from the photosynthetic water-oxidizing complex reveals photooxidation of a protein residue, Biochemistry 30 (1991) 4740–4747.
[22] T. Ono, Y. Inoue, Abnormal redox reactions in photosynthetic O_2-evolving centers in NaCl/EDTA-washed PS II—A dark-stable EPR multiline signal and an unknown positive charge accumulator, Biochim. Biophys. Acta 1020 (1990) 269–277.
[23] A. Boussac, A.W. Rutherford, Nature of the inhibition of the oxygen-evolving enzyme of Photosystem-II induced by NaCl washing and reversed by the addition of Ca^{2+} or Sr^{2+}, Biochemistry 27 (1988) 3476–3483.
[24] A. Boussac, J.L. Zimmermann, A.W. Rutherford, EPR signals from modified charge accumulation states of the oxygen evolving enzyme in Ca^{2+}-deficient Photosystem II, Biochemistry 28 (1989) 8984–8989.
[25] A. Boussac, J.L. Zimmermann, A.W. Rutherford, J. Lavergne, Histidine oxidation in the oxygen-evolving Photosystem-II enzyme, Nature 347 (1990) 303–306.
[26] C. Berthomieu, A. Boussac, Histidine oxidation in the S_2 to S_3 transition probed by FTIR difference spectroscopy in the Ca^{2+}-depleted Photosystem-II—Comparison with histidine radicals generated by UV irradiation, Biochemistry 34 (1995) 1541–1548.
[27] B.J. Hallahan, J.H.A. Nugent, J.T. Warden, M.C.W. Evans, Investigation of the origin of the S3 EPR signal from the oxygen-evolving complex of Photosystem 2—The role of Tyrosine-Z, Biochemistry 31 (1992) 4562–4573.
[28] M.L. Gilchrist, J.A. Ball, D.W. Randall, R.D. Britt, Proximity of the manganese cluster of Photosystem-II to the redox-active tyrosine Y-Z, Proc. Natl. Acad. Sci. U. S. A. 92 (1995) 9545–9549.
[29] D.A. Force, D.W. Randall, R.D. Britt, Proximity of acetate, manganese, and exchangeable deuterons to tyrosine $Y_Z^{\cdot}$ in acetate-inhibited Photosystem II membranes: implications for the direct involvement of $Y_Z^{\cdot}$ in water-splitting, Biochemistry 36 (1997) 12062–12070.
[30] X.S. Tang, D.W. Randall, D.A. Force, B.A. Diner, R.D. Britt, Manganese–tyrosine interaction in the Photosystem II oxygen-evolving complex, J. Am. Chem. Soc. 118 (1996) 7638–7639.
[31] A.V. Astashkin, H. MIno, A. Kawamori, T.A. Ono, Pulsed EPR study of the $S_2^{\cdot}$signal in the Ca^{2+}-depleted Photosystem II, Chem. Phys. Lett. 272 (1997) 506–516.
[32] H. Mino, A. Kawamori, T. Ono, Pulsed EPR studies of doublet signal and singlet-like signal in oriented Ca^{2+}-depleted PSII membranes: location of the doublet signal center in PS II, Biochemistry 39 (2000) 11034–11040.
[33] H. Mino, A. Kawamori, T. Matsukawa, T. Ono, Light-induced high-spin signals from the oxygen evolving center in Ca^{2+}-depleted Photosystem II studied by dual mode electron paramagnetic resonance spectroscopy, Biochemistry 37 (1998) 2794–2799.
[34] H. Mino, A. Ishii, T.A. Ono, Nonlineal relationship between g=2 doublet and multiline signals in Ca^{2+}-depleted Photosystem II, Biochim. Biophys. Acta 1606 (2003) 127–136.

[35] D.A. Berthold, G.T. Babcock, C.F. Yocum, A highly resolved, oxygen-evolving Photosystem-II preparation from spinach thylakoid membranes-EPR and electron-transport properties, FEBS Lett. 134 (1981) 231–234.
[36] T. Ono, Y. Inoue, Effects of removal and reconstitution of the extrinsic 33-KDa, 24-KDa and 16-KDa proteins on flash oxygen yield in Photosystem-II particles, Biochim. Biophys. Acta 850 (1986) 380–389.
[37] T. Ono, Y. Inoue, Removal of Ca by pH 3.0 treatment inhibits S_2 to S_3 transition in photosynthetic oxygen evolution system, Biochim. Biophys. Acta 973 (1989) 443–449.
[38] Y. Kodera, H. Hara, A.V. Astashkin, A. Kawamori, T.A. Ono, EPR study of trapped tyrosine Z^+ in Ca-depleted Photosystem-II, Biochim. Biophys. Acta 1232 (1995) 43–51.
[39] H. Mino, A. Kawamori, T. Ono, pH-dependent characteristics of Y_Z radical in Ca^{2+}-depleted Photosystem II studied by CW-EPR and pulsed ENDOR, Biochim. Biophys. Acta 1457 (2000) 157–165.
[40] H. Mino, A.V. Astashkin, A. Kawamori, An EPR and pulsed ENDOR study of the structure of tyrosine $Z^{\bullet}$ in tris-treated Photosystem II, Spectrochim. Acta, A Mol. Spectrosc. 53 (1997) 1465–1483.
[41] D.J. Maclachlan, J.H.A. Nugent, Investigation of the S3 electron paramagnetic resonance signal from the oxygen-evolving complex of Photosystem 2—Effect of inhibition of oxygen evolution by acetate, Biochemistry 32 (1993) 9772–9780.
[42] D.J. Maclachlan, J.H.A. Nugent, J.T. Warden, M.C.W. Evans, Investigation of the ammonium-chloride and ammonium acetate inhibition of oxygen evolution by Photosystem-II, Biochim. Biophys. Acta 1188 (1994) 325–334.
[43] V.A. Szalai, G.W. Brudvig, Reversible binding of nitric oxide to tyrosyl radicals in Photosystem II. Nitric oxide quenches formation of the S3 EPR signal species in acetate-inhibited Photosystem II, Biochemistry 35 (1996) 15080–15087.
[44] A. Bencini, D. Gatteschi, Electron Paramagnetic Resonance of Exchange Coupled Systems, Springer-Verlag, New York, 1990.
[45] M. Baumgarten, J.S. Philo, G.C. Dismukes, Mechanism of photoinhibition of photosynthetic water oxidation by Cl^- depletion and F^- substitution-oxidation of a protein residue, Biochemistry 29 (1990) 10814–10822.
[46] T.A. Ono, Y. Inoue, A marked upshift in threshold temperature for the S_1 to S_2 transition induced by low pH treatment of PS II membranes, Biochim. Biophys. Acta 1015 (1990) 373–377.
[47] J.M. Peloquin, K.A. Campbell, R.D. Britt, Mn-55 pulsed ENDOR demonstrates that the Photosystem II "split" EPR signal arises from a magnetically-coupled mangano–tyrosyl complex, J. Am. Chem. Soc. 120 (1998) 6840–6841.
[48] M. Haumann, A. Mulkidjanian, W. Junge, Tyrosine-Z in oxygen-evolving Photosystem II: a hydrogen-bonded tyrosinate, Biochemistry 38 (1999) 1258–1267.